

## Articles

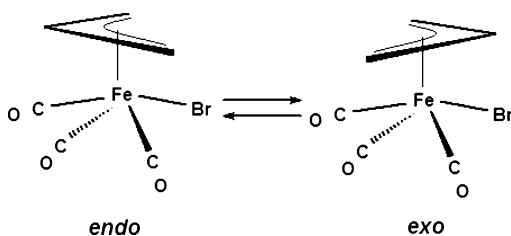
Matrix Photolysis of Fe(allyl)(CO)<sub>3</sub>Br. Evidence for an Unexpected Alternative Mechanism for Allyl RotationThomas E. Bitterwolf<sup>\*,†</sup> and James R. Jeitler<sup>‡</sup>

Department of Chemistry, University of Idaho, Moscow, Idaho 83844-2343, and Division of Natural Sciences and Mathematics, North Idaho College, Coeur d'Alene, Idaho 83814

Received July 5, 2005

Matrix photolysis of a mixture of *endo*- and *exo*-Fe( $\eta^3$ -C<sub>3</sub>H<sub>5</sub>)(CO)<sub>3</sub>Br yields the C<sub>1</sub>-*mer* isomer at visible wavelengths and CO-loss species with UV photolysis. It is proposed that the C<sub>1</sub>-*mer* isomer arises from a Bailar twist. A second Bailar twist completes the allyl pseudorotation.

The pseudorotation of  $\eta^3$ -allyl ligands has been explored since the very early days of organometallic chemistry with notable examples being CpMo(CO)<sub>2</sub>( $\eta^3$ -allyl)<sup>1</sup> and CpRu(CO)( $\eta^3$ -allyl).<sup>2</sup> Limberg et al.<sup>3</sup> and Bitterwolf<sup>4</sup> have examined the photochemical initiation of allyl rotation of CpMo(CO)<sub>2</sub>( $\eta^3$ -allyl), and we have recently described a similar photochemical process for CpRu(CO)( $\eta^3$ -allyl) and ( $\eta^3$ -allyl)Fe(CO)<sub>2</sub>(NO).<sup>5</sup> In all cases, the assumption is made that the allyl ligand rotates about its center of mass while retaining the *syn/anti* protons of the CH<sub>2</sub> groups in a fixed orientation, as is consistent with NMR studies. The results presented here suggest that in at least some cases this simplistic interpretation of the mechanism of pseudorotation may have to be revisited.



The existence of two rotameric isomers for the ( $\eta^3$ -allyl)Fe(CO)<sub>3</sub>Br derivatives was discovered by Nesmeyanov and co-workers on the basis of there being two sets of resonances

\* To whom correspondence should be addressed. E-mail: bitterte@uidaho.edu.

† University of Idaho.

‡ North Idaho College.

(1) (a) Faller, J. W.; Whitmore, B. C. *Organometallics* **1986**, *5*, 752–755. (b) Faller, J. W.; Jakubowski, J. *Organomet. Chem.* **1971**, *31*, C75–C78. (c) Faller, J. W.; Incorvia, M. L. *Inorg. Chem.* **1968**, *7*, 840–842. (d) Davidson, A.; Rode, W. C. *Inorg. Chem.* **1967**, *6*, 2124–2125.

(2) (a) Worley, S. D.; Gibson, D. H.; Hsu, W.-L. *Organometallics* **1982**, *1*, 134–137. (b) Gibson, D. H.; Hsu, W.-L.; Steinmetz, A. L.; Johnson, B. V. *J. Organomet. Chem.* **1981**, *208*, 89–102. (c) Faller, J. W.; Johnson, B. V.; Dryja, T. P. *J. Organomet. Chem.* **1974**, *65*, 395–400.

(3) Limberg, C.; Downs, A. J.; Greene, T. M.; Wistuba, T. *Eur. J. Inorg. Chem.* **2001**, 2613–2618.

(4) Bitterwolf, T. E.; Bays, J. T.; Scallorn, B.; Weiss, C. A.; George, M. W.; Virrels, I. G.; Linehan, J. C.; Yonker, C. R. *Eur. J. Inorg. Chem.* **2001**, 2619–2624.

(5) Bitterwolf, T. E. *Inorg. Chem. Commun.* **2004**, *7*, 956–959.

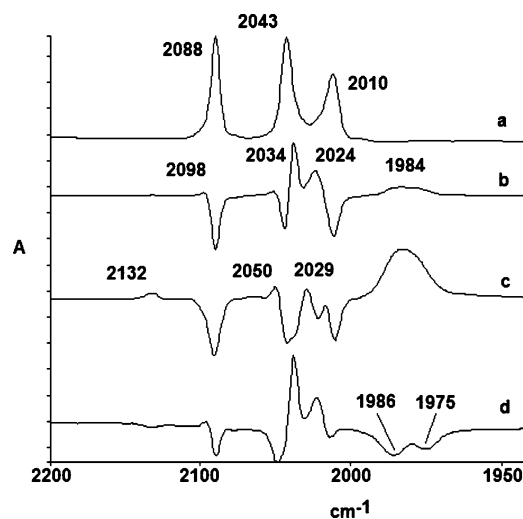


**Figure 1.** Photolysis of Fe( $\eta^3$ -C<sub>3</sub>H<sub>5</sub>)(CO)<sub>3</sub>Br in Nujol, ca. 90 K: (a) before photolysis (absorbance range, 112–0.0 mA); (b) difference spectrum of 10 min photolysis,  $\lambda_{\text{irr}} = 400 \pm 35$  nm – spectrum a (absorbance range, 54 to –55 mA); (c) difference spectrum of 10 min photolysis,  $330$  nm <  $\lambda_{\text{irr}} < 400$  nm – 10 min photolysis,  $\lambda_{\text{irr}} = 450 \pm 35$  nm (absorbance range, 7.4 to –7.2 mA); (d) back photolysis difference spectrum, 10 min photolysis,  $\lambda_{\text{irr}} = 550 \pm 35$  nm – 10 min photolysis,  $\lambda_{\text{irr}} = 400 \pm 35$  nm (absorbance range, 3.0 to –1.2 mA).

for the allyl ligands in these compounds.<sup>6</sup> Faller and Adams<sup>7</sup> carried out detailed NMR studies, which established that the interconversion of the two forms takes place by pseudorotation of the  $\eta^3$ -allyl group; that is, the relative orientation of the *syn* and *anti* protons of the CH<sub>2</sub> groups does not change when the orientation of the allyl changes within the molecule. NMR was essential for these studies, as the IR bands of the two isomers differ by only a few cm<sup>-1</sup>.

Wuu and Wrighton examined the room-temperature solution photolysis of ( $\eta^3$ -C<sub>3</sub>H<sub>5</sub>)Fe(CO)<sub>3</sub>Br in the course of a detailed

(6) Nesmeyanov, A. N.; Kritskaya, I. I. *J. Organomet. Chem.* **1968**, *14*, 387–394. (b) Nesmeyanov, A. N.; Ustynuk, Yu. A.; Kritskaya, I. I.; Shchembelov, G. A. *J. Organomet. Chem.* **1968**, *14*, 395–403.

(7) Faller, J. W.; Adams, M. A. *J. Organomet. Chem.* **1979**, *170*, 71–80.

**Table 1.** Calculated and Observed Carbonyl Stretching Frequencies ( $\text{cm}^{-1}$ ) for  $\text{Fe}(\eta^3\text{-allyl})(\text{CO})_3\text{Br}$  Isomers<sup>a</sup>

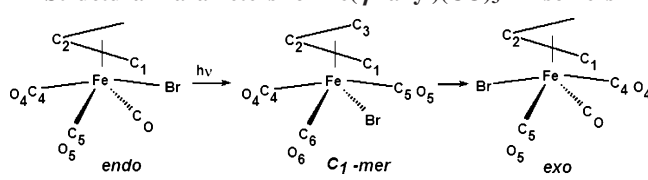
observed, Nujol ca. 90 K		calcd RB3LYP/6-31G**		
endo/exo	$C_1$ isomer	endo	$C_1\text{-mer}$	exo
2088 (1.00)	2098 (0.07)	2173 (0.76)	2177 (0.13)	2173 (0.79)
2043 (1.00)	2034 (1.00)	2137 (1.00)	2134 (1.00)	2137 (1.00)
2010 (0.63)	2024 (0.47)	2115 (0.76)	2127 (0.54)	2116 (0.78)

<sup>a</sup> Relative intensities are presented in parentheses.

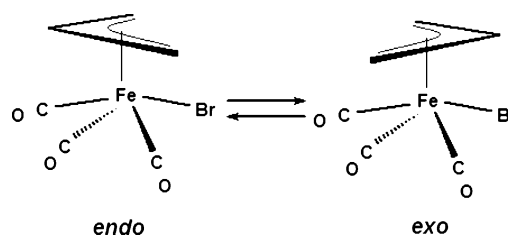
examination of the photochemistry of  $(\eta^3\text{-C}_3\text{H}_5)\text{Ru}(\text{CO})_3\text{Br}$ .<sup>8</sup> It was found that near-UV irradiation of both compounds in 3-methylpentane solution resulted in conversion of the *endo* isomer to the *exo* isomer.

For our photolysis study we chose the readily available  $(\eta^3\text{-C}_3\text{H}_5)\text{Fe}(\text{CO})_3\text{Br}$ , **I**, which is easily soluble in hydrocarbons. Petroleum ether solutions of this compound have electronic bands at 298 nm ( $\epsilon = 1200$ ) and 404 nm ( $\epsilon = 670$ ) and a tail that extends across the visible spectrum. The IR spectrum of **I** in frozen Nujol at ca. 90 K, Figure 1a, has three terminal carbonyl bands at 2088, 2043, and 2010  $\text{cm}^{-1}$ , consistent with the  $C_s$  symmetry of the molecule. The bands of the *endo* and *exo* rotamers are not resolved. Spectral changes were observed upon relatively low energy visible photolysis,  $\lambda_{\text{irr}} = 500 \pm 35$ , with the extent of photolysis increasing with increasing energy. For example, Figure 1b presents the difference spectrum for the photolysis of **I** at  $\lambda_{\text{irr}} = 400 \pm 35$  nm, showing the bleaching of the bands of **I** and growth of new bands at 2098, 2034, and 2024  $\text{cm}^{-1}$  and a broad band at 1984  $\text{cm}^{-1}$ . A small band at 2132  $\text{cm}^{-1}$  characteristic of free CO can be observed. As neither the 2132  $\text{cm}^{-1}$  band nor the broad 1984  $\text{cm}^{-1}$  band is observed at lower energy, we attribute these bands to CO-loss species that become more prevalent with increasing energy. Absorbance changes indicate that almost 50% of the sample is transformed at  $\lambda_{\text{irr}} = 400 \pm 35$  nm. Increasing the energy of the incident radiation into the UV,  $300 \text{ nm} < \lambda_{\text{irr}} < 400 \text{ nm}$ , Figure 1c, results in loss of the bands at 2098, 2034, and 2024  $\text{cm}^{-1}$  as well as starting material bands and growth of the 2132  $\text{cm}^{-1}$  band, the broad, low-energy band, and small bands at 2050 and 2029  $\text{cm}^{-1}$ . By comparison with the absorbance changes in the visible spectrum, these UV changes transform only about 7% of the sample. Back photolysis ( $\lambda_{\text{irr}} = 550 \pm 35$  nm), Figure 1d, reverses this last process, as evidenced by the negative 2132  $\text{cm}^{-1}$  band, although it is interesting to note that photolysis of **I** to give **II** continues even at this remarkably low energy. Of particular note in the back photolysis is the clear resolution of the broad, low-energy band into two distinct bands at 1986 and 1975  $\text{cm}^{-1}$ .

The observed photochemistry consists of two events. Visible photolysis of **I** gives rise a new tricarbonyl species, **II**, which we assume to be the hitherto unobserved  $C_1\text{-mer}$  isomer of  $(\eta^3\text{-C}_3\text{H}_5)\text{Fe}(\text{CO})_3\text{Br}$  with IR bands at 2098, 2034, and 2024  $\text{cm}^{-1}$ . UV photolysis results in loss of CO by species **II** and *endo*- or *exo*-**I**, giving rise to the broad, non-Gaussian band at 1984  $\text{cm}^{-1}$  as well as smaller bands at 2050 and 2029  $\text{cm}^{-1}$ . *endo*- and *exo*-**I** may each give rise to two isomeric dicarbonyl photo-products in which the carbonyl ligands are oriented *cis* to one another, while the  $C_1\text{-mer}$  isomer may give rise to three CO-loss isomers, one of which has a pair of *trans* carbonyl ligands. Given that there may be as many as seven CO-loss isomers, the back photolysis bleaching of only a subset of these (bands at 1986 and 1975  $\text{cm}^{-1}$ ) seemingly related to the  $C_1\text{-mer}$  species is unusual and may be attributable to the higher energy of the  $C_1\text{-mer}$  species itself.

**Table 2.** Experimental and Calculated (BP3LYP/6-31G\*\*) Structural Parameters for  $\text{Fe}(\eta^3\text{-allyl})(\text{CO})_3\text{Br}$  Isomers


	<i>endo</i> - $\text{Fe}(\eta^3\text{-allyl})(\text{CO})_3\text{Br}$		$C_1\text{-mer}$	<i>exo</i>
	crystal structure	calcd	calcd	calcd
Bond Lengths (Å)				
Fe–Br	2.494(2)	2.555	2.486	2.538
Fe–C1	2.126(8)	2.144	2.121	2.160
Fe–C2	2.058(11)	2.112	2.101	2.103
Fe–C3			2.189	
Fe–C4	1.791(12)	1.776	1.829	1.778
Fe–C5	1.785(9)	1.807	1.833	1.806
Fe–C6			1.786	
C4–O4	1.123(12)	1.149	1.145	1.149
C5–O5	1.150(12)	1.145	1.144	1.145
C6–O6			1.148	
C1–C2	1.392(10)	1.408	1.414	1.407
C2–C3			1.403	
Bond Angles (deg)				
Br–Fe–C1	88.3(2)	88.11		99.71
Br–Fe–C2	105.2(4)	104.74		84.34
Br–Fe–C4	171.9(4)	170.57	82.97	171.42
Br–Fe–C5	83.5(2)	80.95	82.66	83.55
Br–Fe–C6			98.97	
Fe–C4–O4	177.8(11)	178.43	177.29	179.11
Fe–C5–O5	177.8(11)	178.28	178.01	177.96
Fe–C6–O6			176.30	
C4–Fe–C5	91.6(3)	93.21	165.60	93.46
C4–Fe–C6			91.50	
C5–Fe–C5'	105.9(4)	102.63		102.49
C5–Fe–C6			91.70	
C1–C2–C3	124.1(4)	122.77	121.75	122.71

**Scheme 1**

DFT calculations (Spartan 04, ver. 1.0.3) at the RB3LYP level using the 6-31G\*\* basis set were carried out for the *endo*, *exo*, and  $C_1\text{-mer}$  isomers. The computed values for the carbonyl frequencies, Table 1, are shifted about 100  $\text{cm}^{-1}$  to higher energy relative to the observed bands, but the pattern of the three sets of calculated bands almost perfectly matches the observed patterns. The computed electronic excitation bands have maxima at 394 and 305 nm (*endo*) and 401 and 312 nm (*exo*), in remarkable, and certainly fortuitous, agreement with the observed spectra. Bond lengths and angles for the three computed conformations and for the known molecular structure of *endo*- $(\eta^3\text{-allyl})\text{Fe}(\text{CO})_3\text{Br}$ <sup>9</sup> are presented in Table 2. The agreement between the computed and observed structure is very good.

Treating **I** as an octahedral complex, the transformation of **I** to **II** requires a rearrangement of the carbonyl ligand set from a facial to a meridional arrangement. Such transformations are well known in coordination chemistry, where mechanisms involving either  $D_{3h}$  intermediates (Bailar twist<sup>10</sup>) or a bicapped

(8) Wu, Y.-M.; Wrighton, M. S. *Organometallics* **1988**, *7*, 1839–1845.

(9) Simon, F. E.; Lauher, J. W. *Inorg. Chem.* **1980**, *19*, 2338–2343.

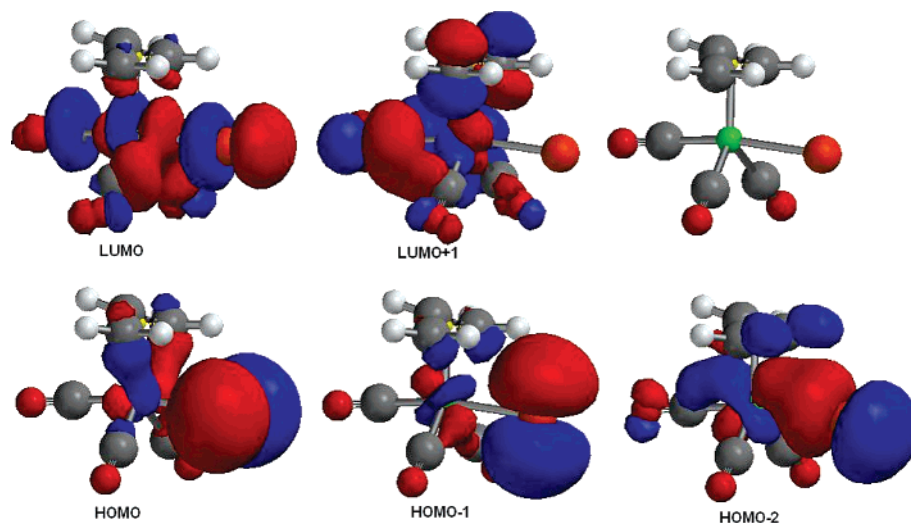
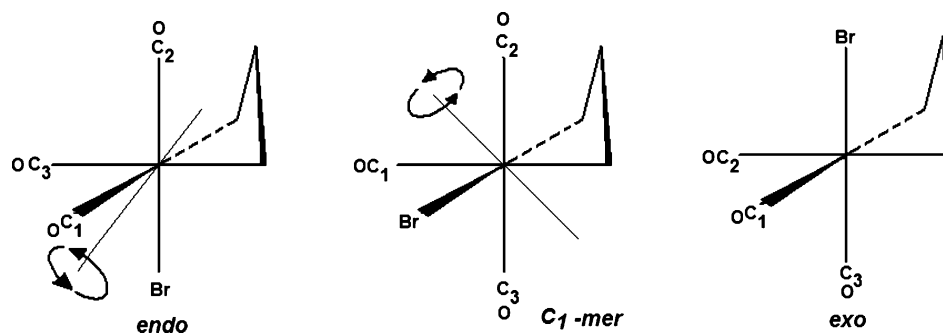


Figure 2. Kohn–Sham orbitals for  $\text{endo}-(\eta^3\text{-C}_3\text{H}_5\text{Fe}(\text{CO})_3\text{Br})$ .

Scheme 2. Proposed Mechanism for Allyl Pseudorotation of  $\text{Fe}(\eta^3\text{-C}_3\text{H}_5)(\text{CO})_3\text{Br}$  Utilizing a Series of Bailar Twists



tetrahedron (Ray–Dutt twist<sup>11</sup>) have been invoked. Several workers have examined the theoretical underpinnings of these rearrangement mechanisms.<sup>12</sup> Assuming a Bailar twist mechanism in the current case, Scheme 1, transformation of *endo*-I to **II** requires one Bailar twist, while transformation of **II** to *exo*-I simply requires a second. If we make the reasonable assumption that photochemically generated **II** is energetically higher than either *endo*-I or *exo*-I, a Bailar twist to either of these would be spontaneous at room temperature. Hence the *endo* to *exo* pseudorotation observed by Wu and Wrighton need only generate **II** photochemically for the rotation to take place.

Examination of the Kohn–Sham orbitals arising from our DFT calculations, Figure 2, provides a useful insight into the nature of the highest occupied and lowest unoccupied molecular orbitals. The nearly degenerate HOMO and HOMO–1 orbitals, –6.80 and –6.81 eV, respectively, are dominantly associated with the nonbonding orbitals of the bromide ligand, while the much lower HOMO–2, –7.80 eV, appears to correspond to a significant Fe–Br bonding component. The LUMO orbital, –2.08 eV, has  $\sigma$ -antibonding interactions with both the bromide and carbonyl *trans* to the bromide. The very much higher energy LUMO+1, –1.46 eV, exhibits antibonding interactions between the metal and allyl ligand, although the dominant contribution is toward the Fe–CO back-bond. The HOMO–LUMO transi-

tion appears to be a ligand nonbonding orbital to metal charge transfer in which the bonds to the *trans*-oriented carbonyl and bromide ligands in the excited state are weakened, facilitating the observed rearrangement. The remarkably good correlation between the calculated electronic spectrum, which predicts bands at 401 and 312 nm, and the observed spectrum with bands at 404 and 298 nm suggests that the energies of the HOMO/LUMO gap are at least consistent with experiment.

The Bailar twist has been proposed to explain the photochemical conversion of  $\Lambda$ -*fac*-Cr(S-trp)<sub>3</sub> to  $\Delta$ -*fac*-Cr(S-trp)<sub>3</sub>, where S-trp is the bidentate amino acid ligand (*S*)-tryptophanato,<sup>13</sup> as well as the deracemization of chromium oxalate and acac complexes with circularly polarized light.<sup>14</sup> A very similar thermal process involving  $(\eta^3\text{-C}_3\text{H}_5)\text{Mo}(\text{CO})_2(\text{diphos})\text{Cl}$  has been described by Faller et al.<sup>15</sup> It is difficult to imagine how an analogous process might account for the *endo* to *exo* rotations of allyl groups in the formally seven-coordinate group VI  $(\eta^5\text{-C}_5\text{H}_5)\text{M}(\text{CO})_2(\eta^3\text{-C}_3\text{H}_5)$  compounds, but a “rotation” in the formally five-coordinate  $(\eta^3\text{-C}_3\text{H}_5)\text{Fe}(\text{CO})_2(\text{NO})$  compounds might pass through a square pyramidal or trigonal bipyramidal intermediate. Lin and co-workers have recently described the results of theoretical studies of allyl rearrangements on a number

(10) Bailar, J. C., Jr. *J. Inorg. Nuc. Chem.* **1958**, *8*, 165–175.

(11) Ray, P.; Dutt, N. K. *J. Indian Chem. Soc.* **1943**, *20*, 81–92.

(12) (a) Casanova, D.; Cirera, J.; Lluell, M.; Alemany, P.; Avnir, D.; Alvarez, S. *J. Am. Chem. Soc.* **2004**, *126*, 1755–1763. (b) Hansen, L. M.; Marynick, D. S. *Inorg. Chem.* **1990**, *29*, 2482–2486. (c) King, R. B. *THEOCHEM* **1989**, *185*, 15–37. (d) Hoffmann, R. H.; Howell, J. M.; Rossi, A. R. *J. Am. Chem. Soc.* **1976**, *98*, 2484–2492. (e) Muetterties, E. L. *J. Am. Chem. Soc.* **1968**, *90*, 5097–5102.

(13) Kane-Mcguire, N. A. P.; Hanks, T. W.; Jurs, D. G.; Tollison, R. M.; Heatherington, A. L.; Ritzenhalter, L. M.; McNulty, L. M.; Wilson, H. M. *Inorg. Chem.* **1995**, *34*, 1121–1124.

(14) (a) Stevenson, K. L.; Sievers, R. E. *Inorg. Chem.* **1976**, *15*, 1086–1088. (b) Stevenson, K. L.; Vaden Driesche, T. P. *J. Am. Chem. Soc.* **1974**, *96*, 7964–7968. (c) Yoneda, H.; Nakashimi, Y.; Sakaguchi, U. *Chem. Lett.* **1973**, 1343–1346. (d) Stevenson, K. L. *J. Am. Chem. Soc.* **1972**, *94*, 6652–6654. (e) Stevenson, K. L.; Verdieck, J. F. *J. Am. Chem. Soc.*, **1968**, *90*, 2974–2975.

(15) Faller, J. W.; Haitko, D. A.; Adams, R. D.; Chodosh, D. F. *J. Am. Chem. Soc.* **1977**, *99*, 1654–1655.

of CpM( $\eta^3$ -allyl) compounds<sup>16</sup> and, of more immediate relevance, on ( $\eta^3$ -allyl)Ru(CO)(PH<sub>3</sub>)<sub>2</sub>Cl.<sup>17</sup> For the ruthenium compound they found an energetically reasonable mechanism involving  $\eta^3$ - $\eta^1$  transformations and were unable to locate a pathway for simple rotation of the allyl unit. A Bailar twist pathway was not investigated. We cannot rule out an  $\eta^3$ - $\eta^1$  transformation as contributing to *endo* to *exo* transformations in solution, although our DFT studies do not support the involvement of iron-allyl bonding in any of the energetically accessible HOMO or LUMO orbitals.  $\eta^1$ -Allyl groups are rarely observed in matrix photochemistry since the barrier to recomplexation is quite low. In the present case there is no obvious

(16) (a) Ariafard, A.; Bi, S. W.; Lin, Z. Y. *Organometallics* **2005**, *24*, 2241–2244. (b) Bi, S.; Ariafard, A.; Jia, G. C.; Lin, Z. Y. *Organometallics* **2005**, *24*, 680–686.

(17) Xue, P. Bi, S.; Sung, H. H. Y.; Williams, I. D.; Lin, Z.; Jia, G. *Organometallics* **2004**, *32*, 4735–4743.

(18) Murdoch, H. D.; Weiss, E. *Helv. Chim. Acta* **1962**, *45*, 1927–1933.

(19) Bays, J. T.; Bitterwolf, T. E.; Lott, K. A.; Ollino, M. A.; Rest, A. J.; Smith, L. M. *J. Organomet. Chem.* **1998**, *554*, 75–85.

way that a transient  $\eta^1$ -species could give rise to the C<sub>1</sub>-*mer* isomer without substantial reorganization of the ligands in the short-lived five-coordinate  $\eta^1$ -state.

### Experimental Section

Fe( $\eta^3$ -C<sub>3</sub>H<sub>5</sub>)(CO)<sub>3</sub>Br was prepared by the method of Murdoch and Weiss.<sup>18</sup> Details of the photochemical methods have been reported previously.<sup>19</sup> Nujol is degassed by heating under vacuum and stored under nitrogen.

Quantum mechanical calculations were carried out using the Spartan 04, version 1.0.3, software package.

**Acknowledgment.** We thank Idaho INBRE for a summer Visiting Faculty Fellowship (J.R.J.). This research has been generously supported by the National Science Foundation, CHE-0315226. This work was also supported by NIH Grant Number P20 RR16454 from the INBRE Program of the National Center for Research Resources.

OM050558L